Supplemental Materials

Molecular Biology of the Cell

Tan et al.

Supplemental Materials

Figures and Figure Legends

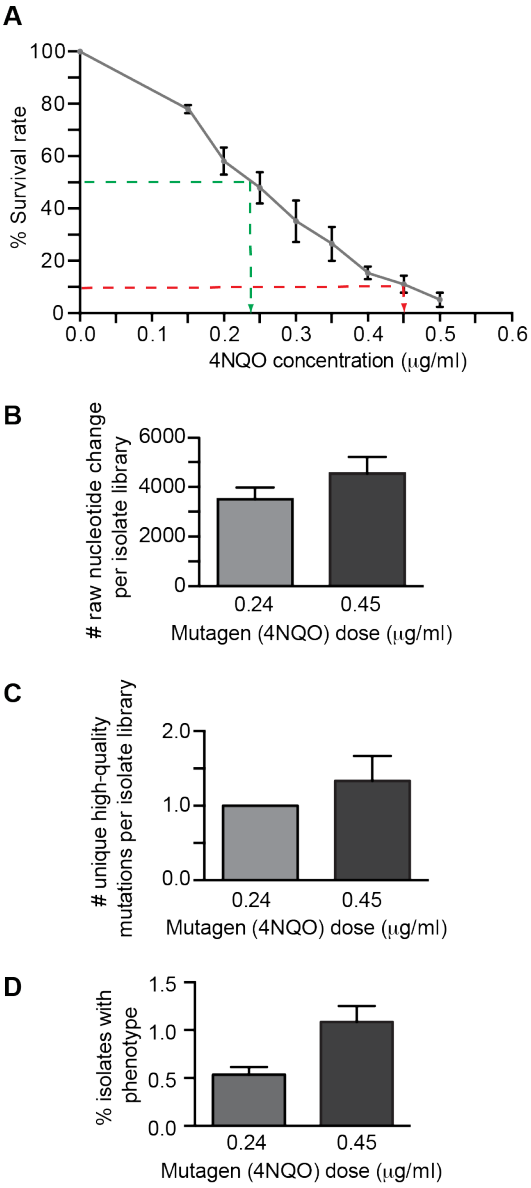

Figure S1. Mutagenesis of *A. nidulans* spores with 4NQO. (A) A graph of the survival rate of *A. nidulans* spores after treatment with increasing amounts of the mutagen 4NQO. The green and red dashed lines indicate 50% and 10% survival rates, respectively (n = 3 independent experiments). Error bars represent SD. (B) A bar graph showing the mean number of raw nucleotide changes per isolate for spores subjected to 0.24 µg/ml (50% survival rate) or 0.45 µg/ml (10% survival rate) 4NQO. The mean ± SEM for spores treated with 0.24 µg/ml or 0.45 µg/ ml 4NQO is 3509.8 ± 464.4 (n = 4 mutants) or 4533.0 ± 675.1 (n = 3 mutants), respectively. The means are not

significantly different ($p = 0.284$, unpaired t-test). (C) A bar graph displaying the mean number of unique high-quality mutations per isolate for spores subjected to either 0.24 µg/ml or 0.45 µg/ml 4NQO. The mean ± SEM for spores subjected to either 0.24 µg/ml or 0.45 µg/ml is 1.0 ± 0.0 ($n = 4$ mutants) or 1.33 ± 0.33 ($n = 3$ mutants), respectively. The means are not significantly different ($p = 0.423$, unpaired t-test). (D) A bar graph displaying the percentage of isolates with a phenotype for spores subjected to either 0.24 µg/ml or 0.45 µg/ml 4NQO. The mean ± SE of the proportion for spores subjected to either 0.24 µg/ml or 0.45 µg/ml is 0.536 ± 0.079 ($n = 8585$ isolates) or 1.086 ± 0.167 ($n = 3871$ isolates) percent, respectively. The higher mutagen dose is more likely to induce a phenotype ($p < 0.001$, two-sample t-test).

A

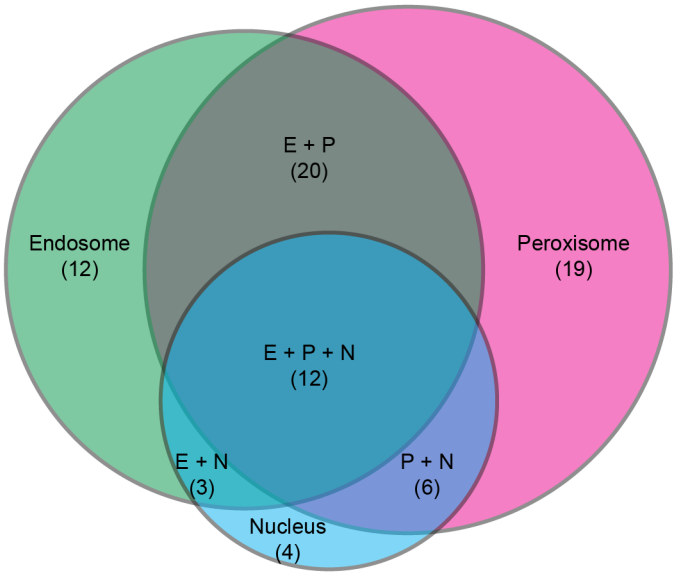

B

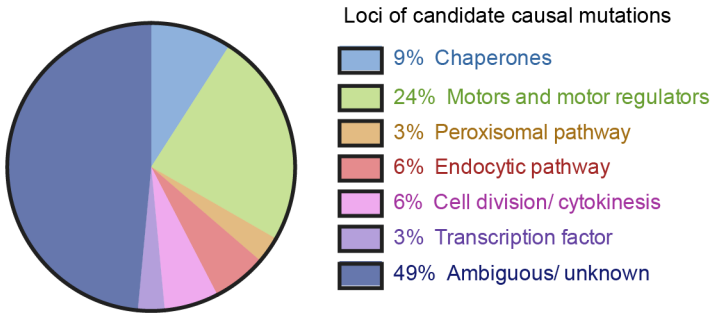

Figure S2. Classification of the hits identified in the screen. (A) A Venn diagram of the 76 hits from the screen showing the number of mutants identified with endosome (E), peroxisome (P), or nuclear (N) distribution phenotypes, or different combinations of each phenotype. (B) A pie chart showing the loci of putative causal mutations identified in the 33 mutants that were sequenced from the screen. “Ambiguous or unknown” refers to hits corresponding to proteins with unknown function or cases in which there was more than one plausible candidate.

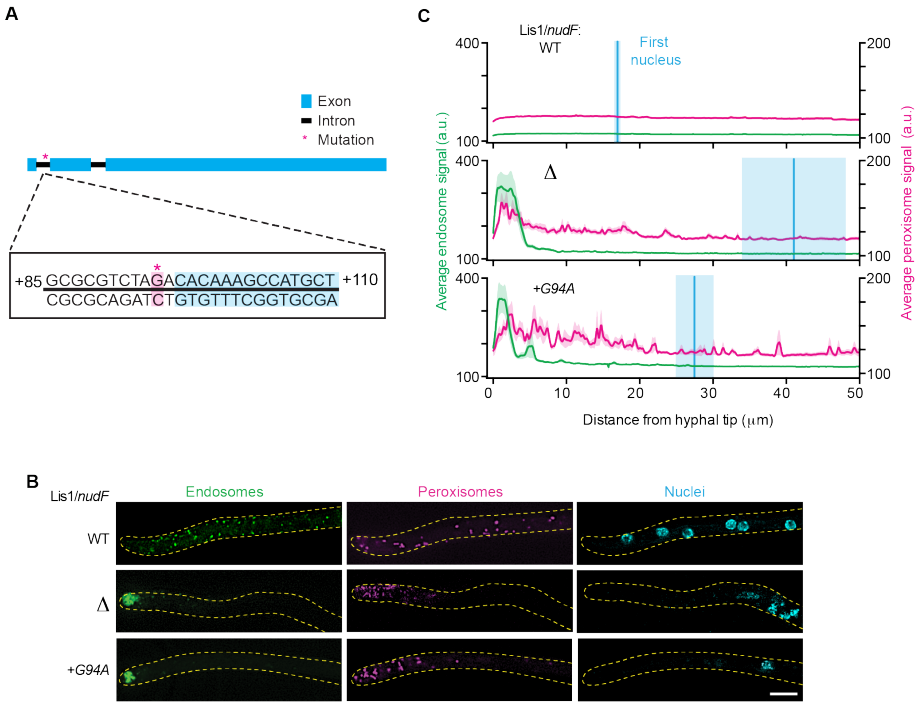

Figure S3. A mutation in the first intron of Lis1 impairs endosome, peroxisome, and nuclear distribution. (A) A cartoon illustrating the position of the nucleotide change identified in the Lis1 gene with the exons, introns, and location of the guanine to adenine nucleotide change (magenta asterisk) at position +94 shown. (B) Representative micrographs of endosomes (green), peroxisomes (magenta), and nuclei (cyan) in wild-type hyphae (top panels), Lis1Δ hyphae (middle panels), and Lis1^{+G94A} hyphae (bottom panels). Scale bar, 5 μm. (C) Endosome, peroxisome, and nuclear distributions were quantified as described in Figure 2D. The mean ± SEM distances from the most distal nucleus to the hyphal tip were 16.95 ± 0.57 μm (n = 52) for wild-type, 41.03 ± 7.24 μm (n = 16) for Lis1Δ, and 27.46 ± 2.71 μm (n = 8) for Lis1^{+G94A} hyphae. The position of the distal nucleus in Lis1Δ and Lis1^{+G94A} hyphae was significantly different from wild-type ($p < 0.006$; unpaired t-test).

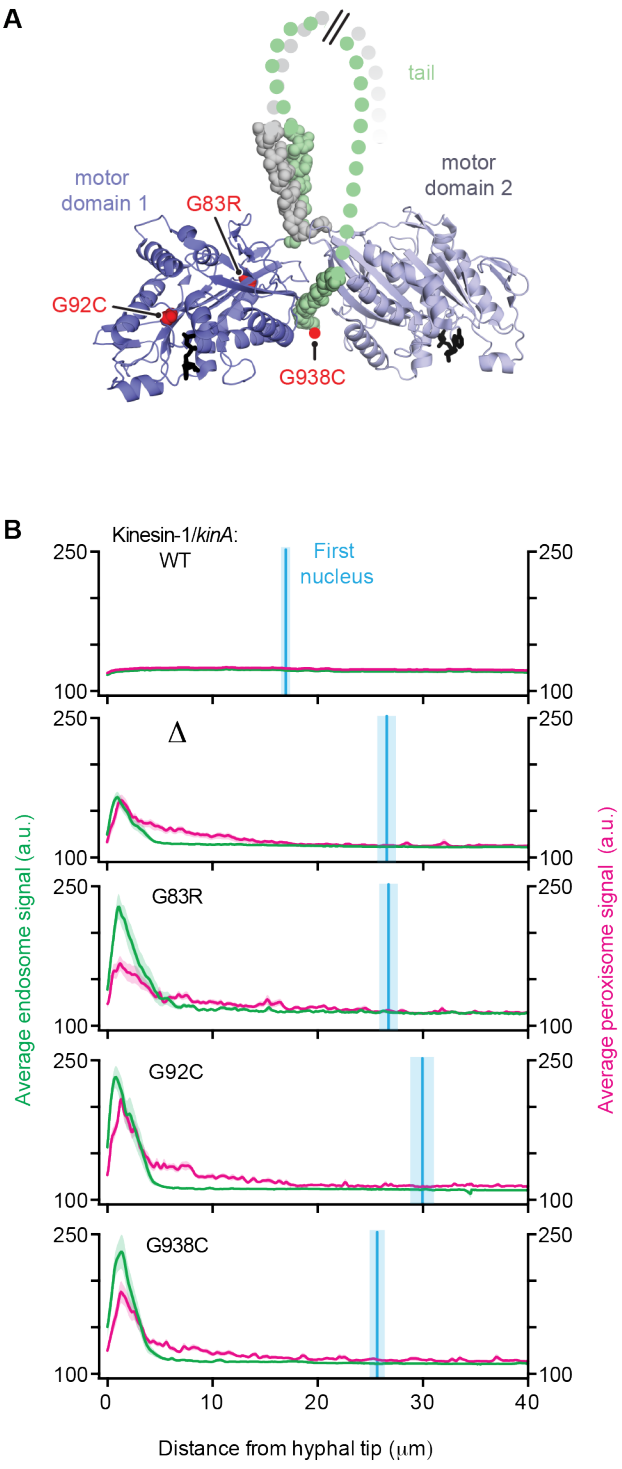

Figure S4. Three kinesin-1 mutations impair endosome, peroxisome, and nuclear distribution. (A) Structure of *Drosophila melanogaster* kinesin-1 (PDB 2Y65, (Kaan *et al.*, 2011)) in the auto-inhibited conformation, with a tail peptide bound between the motor domains, showing the equivalent positions of the three *A. nidulans* kinesin-1 mutations. (B) Endosome, peroxisome, and nuclear distributions were quantified as described in Figure 2D. The mean ± SEM distances from the most distal nucleus to the

hyphal tip were 16.95 ± 0.57 µm (*n* = 52) for wild-type, 26.54 ± 1.01 µm (*n* = 36) for kinesin-1Δ, 26.73 ± 1.02 µm (*n* = 25) for kinesin-1^{G83R}, 29.94 ± 1.24 µm (*n* = 24) for kinesin-1^{G92C}, and 25.65 ± 0.84 µm (*n* = 22) for kinesin-1^{G938C} hyphae. The position of the distal nucleus in all three kinesin-1 mutants and in the kinesin-1 deletion strain were significantly different than wild-type ($p < 0.0001$; unpaired t-test).

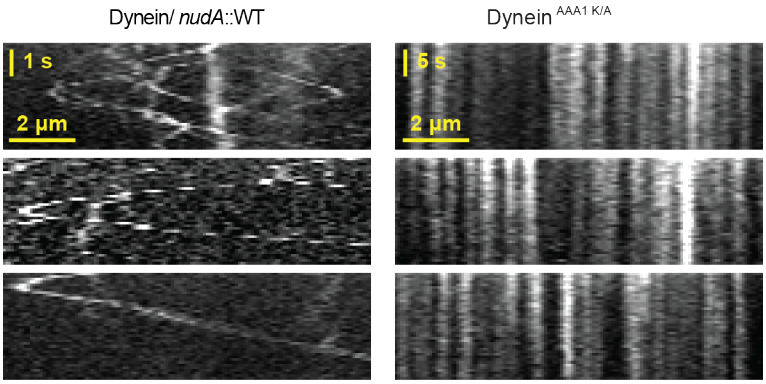

Figure S5. Endosomes are immotile in the dynein$^{AAA1\ K/A}$ mutant. Representative kymographs of TagGFP-Rab5/ RabA-labeled endosome motility in wild-type (left panels) and dynein$^{AAA1\ K/A}$ hyphae (right panels). No directed endosome motility was detected in dynein$^{AAA1\ K/A}$ hyphae, in contrast to the dynein$^{AAA1\ G/C}$ and dynein$^{AAA3\ R/L}$ strains (see Figure 4B).

Supplemental Tables

Supplemental Table 1. *Aspergillus nidulans* strains used in this study. All promoters are the endogenous promoter, unless otherwise stated.

Strain	Genotype	Source
LZ104	[GFP::*nudA*^{K1940A}]; *pyroA4*; *pyrG89*; *nkuAΔ*::*argB*	Zhang et al., 2010
RPA520	*yA*::[*gpdA*(p)::mCherry::FLAG-PTS1::*Afpyro*]; [HH1::TagBFP::*Afribo*]; [TagGFP2::*rabA*::*AfpyrG*]; *pyrG89*; *pyroA4; pabaA1*; *nkuAΔ*::*argB*	This work
RPA643	[*nudF*$^{+G94A}$::*bar*]; *yA*::[*gpdA*(p)::mCherry::FLAG-PTS1::*Afpyro*]; [HH1::TagBFP::*Afribo*]; [TagGFP2::*rabA*::*AfpyrG*]; *pyrG89*; *pyroA4; pabaA1*; *nkuAΔ*::*argB*	This work
RPA672	[*nudKΔ*::*pabaA*]; *yA*::[*gpdA*(p)::mCherry::FLAG-PTS1::*Afpyro*]; [HH1::TagBFP::*Afribo*]; [TagGFP2::*rabA*]; *pyrG89*; *pyroA4; pabaA1*; *nkuAΔ*::*argB*	This work
RPA675	[*nudA*^{R2795L}]; *yA*::[*gpdA*(p)::mCherry::FLAG-PTS1::*Afpyro*]; [HH1::TagBFP::*Afribo*]; [TagGFP2::*rabA*]; *pyrG89*; *pyroA4; pabaA1*; *nkuAΔ*::*argB*	This work
RPA678	[*nudA*^{G1937C}]; *yA*::[*gpdA*(p)::mCherry::FLAG-PTS1::*Afpyro*]; [HH1::TagBFP::*Afribo*]; [TagGFP2::*rabA*]; *pyrG89*; *pyroA4; pabaA1*; *nkuAΔ*::*argB*	This work
RPA693	[*nudK*^{G200W}::*bar*]; *yA*::[*gpdA*(p)::mCherry::FLAG-PTS1::*Afpyro*]; [HH1::TagBFP::*Afribo*]; [TagGFP2::*rabA*::*AfpyrG*]; *pyrG89*; *pyroA4; pabaA1*; *nkuAΔ*::*argB*	This work
RPA720	[*kinA*^{G83R}::*bar*]; *yA*::[*gpdA*(p)::mCherry::FLAG-PTS1::*Afpyro*]; [HH1::TagBFP::*Afribo*]; [TagGFP2::*rabA*::*AfpyrG*]; *pyrG89*; *pyroA4; pabaA1*; *nkuAΔ*::*argB*	This work
RPA722	[*kinA*^{G92C}::*bar*]; *yA*::[*gpdA*(p)::mCherry::FLAG-PTS1::*Afpyro*]; [HH1::TagBFP::*Afribo*]; [TagGFP2::*rabA*::*AfpyrG*]; *pyrG89*; *pyroA4; pabaA1*; *nkuAΔ*::*argB*	This work
RPA723	[*kinA*^{G938C}::*bar*]; *yA*::[*gpdA*(p)::mCherry::FLAG-PTS1::*Afpyro*]; [HH1::TagBFP::*Afribo*]; [TagGFP2::*rabA*::*AfpyrG*]; *pyrG89*; *pyroA4; pabaA1*; *nkuAΔ*::*argB*	This work
RPA727	[*nudFΔ*::*AfpyrG*]; *yA*::[*gpdA*(p)::mCherry::FLAG-PTS1::*Afpyro*]; [HH1::TagBFP::*Afribo*]; [TagGFP2::*rabA*::*AfpyrG*]; *pyrG89*; *pyroA4; pabaA1*; *nkuAΔ*::*argB*	This work
RPA729	[*nudAΔ*::*AfpyrG*]; *yA*::[*gpdA*(p)::mCherry::FLAG-PTS1::*Afpyro*]; [HH1::TagBFP::*Afribo*]; [TagGFP2::*rabA*::*AfpyrG*]; *pyrG89*; *pyroA4; pabaA1*;	This work

RPA735	*nkuAΔ*::*argB* [*kinAΔ*::*Afpyro*]; *yA*::[*gpdA*(p)::mCherry::FLAG-PTS1::*Afpyro*]; [HH1::TagBFP::*Afribo*]; [TagGFP2::*rabA*::*AfpyrG*]; *pyrG89*; *pyroA4*; *nkuAΔ*::*argB*	This work

Supplemental Table 2. *S. cerevisiae* strains used in this study.

Strain	Genotype	Source
RPY753	*MATa; his3-11; 5; ura3-1; leu2-3; 112 ade2-1; trp-1-1; prb1Δ; pac1Δ::klURA3; pep4Δ::HIS5; ndl1Δ::cgLEU2;* P_{GAL1}*-ZZ-Tev-GFP-3xHA-GST-DYN1*$_{331kDa}$*-gs-DHA-Kan*^{R}	Huang et al., 2012
RPY1396	*MATa; his3-11; 5; ura3-1; leu2-3; 112 ade2-1; trp-1-1; prb1Δ; pac1Δ; pep4Δ::HIS5; ndl1Δ::cgLEU2;* P_{GAL1}*-ZZ-Tev-GFP-3XHA-DYN1*$_{331kDa}^{R2620L}$*-gs-DHA-Kan*^{R}	This work
RPY1424	*MATa; his3-11; 5; ura3-1; leu2-3; 112 ade2-1; trp-1-1; prb1Δ; pac1Δ; pep4Δ::HIS5; ndl1Δ::cgLEU2;* P_{GAL1}*-ZZ-Tev-GFP-3XHA-GST-DYN1*$_{331kDa}^{G1799C}$*-gs-DHA-Kan*^{R}	This work